

Preparation and characterization of a novel positively charged nanofiltration membrane based on polysulfone

Ahmad Akbari, Hosna Solymani, Sayed Majid Mojallali Rostami

Institute of Nanoscience and Nanotechnology, University of Kashan, Kashan, Islamic Republic of Iran

Correspondence to: A. Akbari (E-mail: akbari@kashanu.ac.ir)

ABSTRACT: The goal of this study was to prepare positively charged nanofiltration (NF) membranes to remove cations from aqueous solutions. A composite NF membrane was fabricated by the modification of a polysulfone ultrafiltration support. The active top layer was formed by the interfacial crosslinking polymerization of poly(ethylene imine) (PEI) with *p*-xylene dichloride (XDC). Then, it was quaternized by methyl iodide (MI) to form a perpetually positively charged layer. The chemical and morphological changes of the membrane surfaces were studied by Fourier transform infrared spectroscopy, scanning electron microscopy (SEM), and atomic force microscopy. To optimize the membrane operation, the PEI solution concentration, PEI coating time, XDC concentration, crosslinking time, and MI concentration were optimized. Consequently, high water flux ($5.4 \text{ L m}^{-2} \text{ h}^{-1} \text{ bar}^{-1}$) and CaCl_2 rejection (94%) values were obtained for the composite membranes at 4 bars and 30°C . The rejections of the NF membrane for different salt solutions, obtained from pH testing, followed the order $\text{Na}_2\text{SO}_4 < \text{MgSO}_4 < \text{NaCl} < \text{CaCl}_2$. The molecular weight cutoff was calculated by the retention of poly(ethylene glycol) solutions with different molecular weights, and finally, the stoke radius was calculated as 1.47 nm. © 2015 Wiley Periodicals, Inc. *J. Appl. Polym. Sci.* **2015**, *132*, 41988.

KEYWORDS: crosslinking; morphology; nanostructured polymers; separation techniques

Received 10 August 2014; accepted 12 January 2015

DOI: 10.1002/app.41988

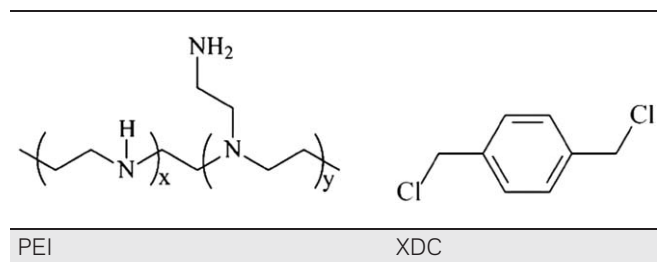
INTRODUCTION

Nanofiltration (NF) is a kind of membrane separation technique, an intermediate ultrafiltration (UF)/reverses osmosis. The transfer mechanism of NF initiates both permeability as in UF and solution–diffusion as in reverse osmosis.¹ NF membranes have advantages, such as a high flux, high retention of multivalent salts, low operation pressure, and low primary investment and operation cost.²

Usually, NF membranes are made by the chemical modification of a UF membrane support.³ NF membranes have a composite structure with a top layer that controls solute transfer and is selective. The selectivity of the top layer in NF membranes is based on the pore size and Donnan exclusion.^{4,5} Most commercially available NF membranes are composite polyamide membranes prepared by the interfacial polymerization of diamines and trimesoyl chloride (TMC). The produced NF membranes usually have a negatively charged separation layer.^{6,7} To improve the separation of cations in aqueous solutions, the membrane surface should have a positive charge. Positively charged modified membranes are useful in the removal of a variety of materials from solutions and also in certain biotechnological applications. For example, positively charged membranes are useful in the removal of endotoxins from solutions. Endotoxins

are toxic substances often derived from bacterial lysates. Conventional methods for NF membrane modification include interfacial polymerization,^{8,9} UV photografting,^{10–12} low-temperature plasma grafting^{13,14} and chemical crosslinking.^{15–17} A few studies have been carried out on positively charged NF membranes. Therefore, it is theoretically and practically important to study the attributes of positively charged NF membranes for the separation of heavy metals. Electrostatic interactions (Donnan repulsion) and the pore radius play important roles in this separation process.

Ruoh *et al.*¹⁸ used interfacial polymerization (IP) to synthesize positively charged NF membranes [poly(ethylene imine) (PEI)/TMC and PEI/terephthaloyl chloride (TPC)] from hyperbranched PEI, which was reacted with two acyl chlorides, TMC and TPC. Those membranes had the same rejection order: $\text{MgCl}_2 > \text{MgSO}_4 > \text{Na}_2\text{SO}_4 > \text{NaCl}$. The PEI/TMC had a higher NaCl rejection than PEI/TPC; however, it had a larger pore size. Du and Zhao¹⁹ fabricated a polysulfone (PSf) composite membrane with a thin, charged layer for NF with the interfacial crosslinking method. The rejection of MgSO_4 in the membrane (1 g/L aqueous solution) was almost 90%, and the rejection of NaCl (1 g/L aqueous solution) was almost 78% at 0.8 MPa and 30°C . Yun *et al.*²⁰ prepared surface-hydrophilized microporous

Table I. Schematic Structures of the Main Materials²⁰

polypropylene membrane via the interfacial crosslinking of PEI. The results for protein filtration suggest that the highly hydrophilic and charged membrane surface was resistant to protein fouling. Lin *et al.*¹² also used crosslinking by *p*-xylylene dichloride (XDC) after UV-induced grafting for quaternization at the surface membrane. In their study, under the optimized preparation conditions, the water flux and MgCl₂ rejection (1 g/L) of the composite membranes reached 60.3 L m⁻² h⁻¹ and 93.2%, respectively.

In this study, an NF membrane was prepared by the coating of PEI on a PSf UF membrane, and then, it was crosslinked by XDC. Afterward, secondary and tertiary amines on the top layer were quaternized by methyl iodide (MI). Finally, the performance of the PEI/PSf NF membranes was characterized with the filtration separation of aqueous feed solutions of CaCl₂, NaCl, MgSO₄, and Na₂SO₄. Additionally, the comparison of the salt rejection and water flux before and after quaternization is illustrated and discussed. The UF PSf membrane was selected as a support membrane because of its good chemical and thermal stability.

EXPERIMENTAL

Materials

PSf (molecular weight = 35 kDa) was manufactured by Aldrich. *N*-Methyl pyrrolidone and poly(ethylene glycol) (PEG; molecular weight = 6 kDa) were purchased from Merck and were used as the solvent and pore former, respectively, in the dope solutions. PEI (average MW = 60 kDa) was purchased as a commercial product, and XDC was obtained from Acros. Pure MI and *n*-heptane were purchased from Merck. Ethanol (96% for washing) and acetone were obtained from Merck (Germany).

Preparation of the PSf Flat-Sheet Supports

A homogeneous dope solution composed of PSf, PEG, and *N*-methyl pyrrolidone (16, 14, and 70% w/w, respectively) was prepared for the fabrication of the UF support membrane. The polymer solution was then cast onto a glass plate with a 256- μ m casting knife applicator. This was followed by immediate immersion in a water coagulant bath at room temperature. The cast membrane was soaked in water for at least 24 h to complete the replacement of water with the solvent available in the membrane pores. The pure-water permeability coefficient for the UF membrane was 840 L m⁻² h⁻¹ bar⁻¹.

Modification of the Membrane Surface

PEI (Table I) is one of the most extensively studied materials in cationic polymer fields.^{21,22} Pure PEI is very effective for the

neutralization of excess anionic colloidal charges, especially under acidic and neutral pH conditions.^{23,24} It is generally believed that the positively charged amine groups in PEI increase the surface charge in the XDC membrane (Table I) and MI, which are applied as crosslinking and quaternization agents. This procedure shows at least two advantages: (1) the resulted hindrance layer is more compact and has a high selectivity, and (2) the membrane surface is positively charged after crosslinking and quaternization.¹²

We prepared the PEI/PSf composite NF membrane by first coating the PEI aqueous solution on the PSf support surface for 1 h and then by drying for 2 h at room temperature. The PEI-coated membrane was immersed into 50 mL of XDC/*n*-heptane solution as a crosslinker with a given concentration. The interfacial crosslinking reaction between PEI and XDC was carried out at room temperature for 5 h. After the crosslinking reaction, the modified membrane was washed with ethanol to remove excess materials. At the next step, the membrane was soaked in a 0.25M NaOH solution to remove H⁺ from the surface. Finally, for the quaternization of PEI on the top layer, the membrane was dipped into a CH₃I solution in ethanol for 2 h. The preparation process of the PEI coating of the PSf membrane is shown schematically in Figure 1.

Chemical and Physical Membrane Characterization

Fourier Transform Infrared (FTIR) Spectroscopy. FTIR spectroscopy (FTIR IBB Bomem MB-100) was used to investigate the surface chemical compositional changes of the PSf membrane before and after modification with the spectra of the wave number ranging from 4000 to 400 cm⁻¹.

SEM. The changes in the surface morphology and cross section of the PSf membranes were evaluated before and after modification by SEM (SEM KYKY-EM 3200, China). To maintain a constant cross-sectional morphology, the membrane samples were broken in liquid nitrogen and then coated with gold before SEM observation.

Atomic Force Microscopy (AFM). AFM images were acquired in tapping mode with silicone-tip cantilevers with a constant force of 40 mN/cm. The mean surface roughness (R_a) was used to express the membrane surface roughness, which was determined by a 5.0 \times 5.0 μ m² area of membrane (scanning probe microscope, NanoScope E). For each membrane, the reported

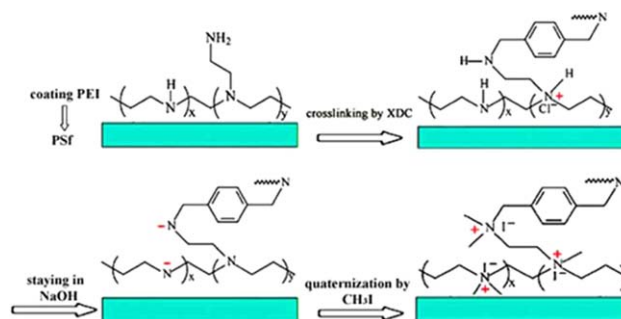


Figure 1. Schematic representation of the preparation of the PSf NF membrane.²⁰ [Color figure can be viewed in the online issue, which is available at wileyonlinelibrary.com.]

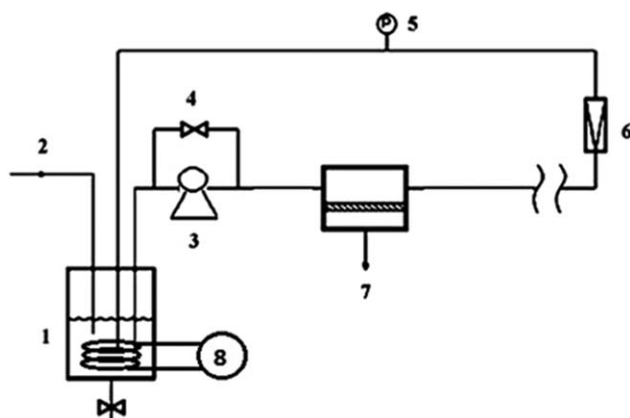


Figure 2. Schematic representation of the NF evaluation cell: (1) feed tank, (2) feed flow, (3) feed pump, (4) bypass, (5) pressure gauge, (6) flow meter, (7) membrane cell, and (8) cooling system.

R_a value was an average of three measurements taken from different regions.

Separation and Permeation Properties

Permeation tests were carried out under a pressure of 4 bar with a flat-sheet, cross-flow NF test cell with a filtration area of 21 cm² (Figure 2). Before the salt solution test, the membrane sample was treated under measurement pressure for 30 min with deionized water. Afterward, the membrane was tested with a salt solution of 1000 ppm. The permeation flux (J_w) was calculated with the following equation:

$$J_w = \frac{\Delta V}{A \times \Delta t} \quad (1)$$

where ΔV is the total volume of the pure water or solution that penetrated through the membrane, A is the membrane area, and Δt is the operation time. The permeability coefficient (L_p) is equal to water flux per effective pressure and is expressed as follows:

$$L_p = \frac{J_w}{\Delta p} \quad (2)$$

The rejection ratio (R ; %) of solute was calculated as follows:

$$R(\%) = \left(1 - \frac{C_p}{C_f}\right) \times 100 \quad (3)$$

where p is operating pressure, C_p and C_f are the solute concentrations in the permeated and feed solution, respectively. The salt concentrations were determined by a bench-top electrical conductivity meter (WTW, Inolab Cond 720 series, Germany).

Molecular Weight Cutoff (MWCO)

The MWCO profile was plotted by the rejection measurement of the PEG solutions with different molecular weights. The PEG concentrations in the feed and permeated solution were measured by IR spectrophotometry.²³ The membrane pore radius was measured on the basis of the PEG molecular weight, which was rejected at 90% by the membrane and was calculated as follows:^{18,25}

$$y = -5 \times 10^{-8} \times x^2 + 5 \times 10^{-4} x + 0.3319 \quad (4)$$

where y is the pore radius (nm) and x is the molecular weight of PEG (g/mol).

RESULTS AND DISCUSSION

Chemical Characterization of the Membrane (FTIR)

The FTIR spectra of the PSf UF membrane [Figure 3(a)] illustrated a characteristic peak at 1585 cm⁻¹, which corresponded to the C=C straining vibration of benzene rings.²⁰ Strong absorptions at 3278 cm⁻¹ were related to N—H stretching and deformation bands of PEI [Figure 3(b,c)].^{7,24} The presence of the aliphatic C—H stretching absorptions (2800–3000 cm⁻¹) was amplified after crosslinking. —NH— reacted, but because of its weak absorption at 1600 cm⁻¹, it was overlapped with the pick of benzene rings available in PSf and XDC.¹² The spectra of the membrane modified by MI did not show obvious changes [compared with Figure 3(d)], except for a stronger peak at 3440 cm⁻¹; this was due to the inevitable adsorption of water by the increased surface charges or the ethanol used as the solvent.

Morphological Characterization of the Membrane

The surface and cross-sectional structure of the PSf membranes before and after modification were examined by SEM (Figures 4 and 5). In Figure 4, all of the SEM images show a similar asymmetric structure with a relatively dense top layer and fingerlike macrovoid support. No significant difference was

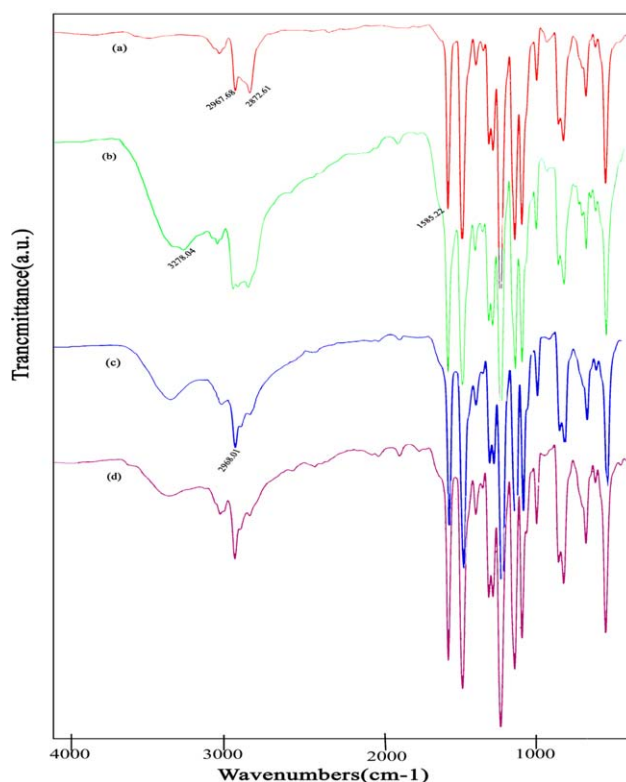


Figure 3. FTIR spectra of the membranes: (a) PSf support membrane, (b) membrane coated with PEI, (c) membrane crosslinked with XDC, and (d) membrane quaternized with MI. [Color figure can be viewed in the online issue, which is available at wileyonlinelibrary.com.]

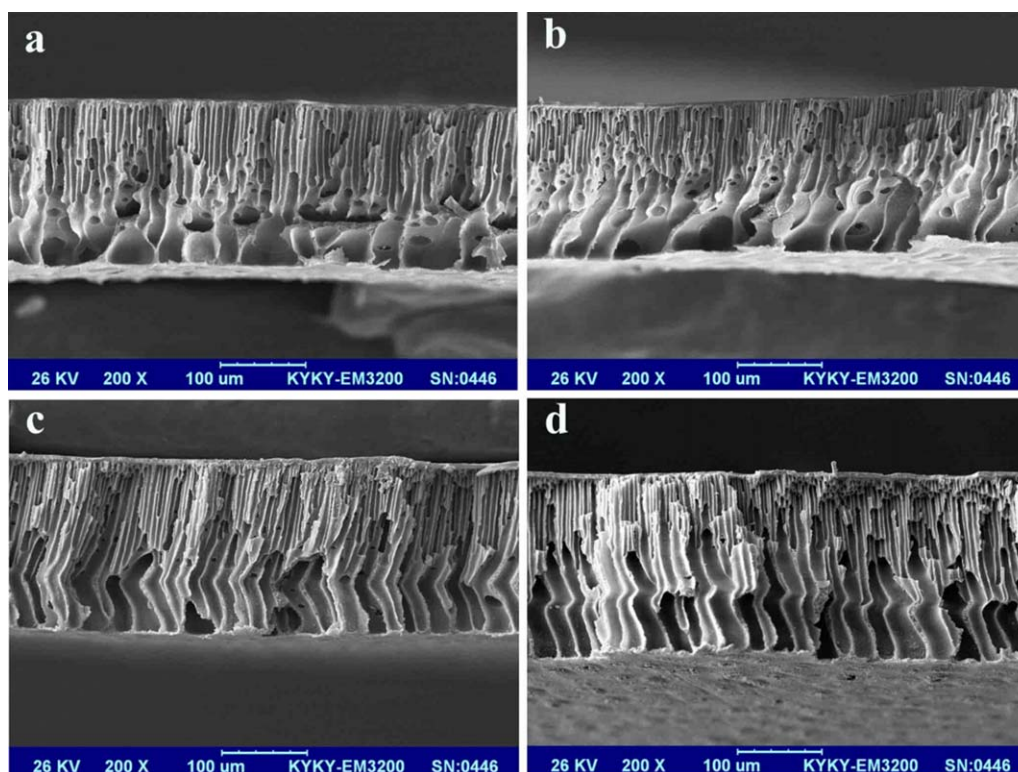


Figure 4. Morphology and structure of the membranes: (a) PSf UF support, (b) membrane coated with PEI, (c) membrane crosslinked with XDC, and (d) NF membrane quaternized with MI. [Color figure can be viewed in the online issue, which is available at wileyonlinelibrary.com.]

observed in the surface morphologies of the PSf support and modified membranes (Figure 5, set 1). Each of the membranes shown had a similar asymmetric structure with a relatively dense top layer and fingerlike macrovoids. The cross section was imaged at $2500\times$ magnification and indicated very little difference between the three membranes after modification. Therefore, the PEI modification layer was thin and certainly less than $3\text{--}4\ \mu\text{m}$; this is typical of that for composite membranes.

Figure 5 (set 2) shows the typical asymmetric structure and fully developed pores. Also, the top layer was recognizable in the crosslinked membrane, with a thickness of $3.75\ \mu\text{m}$ (Figure 5, C_2). After quaternization by MI, the thickness of the top layer increased (Figure 5, D_2). The structure shown for the NF membranes in the SEM images proves that the top layer was formed successfully.

For more investigation of membrane surface on a nanoscale, AFM was applied. Figure 6 shows the AFM images and average surface roughness of the membrane surfaces before [Figure 6(a,b)] and after modification [Figure 6(c,d)]. Figure 6 also illustrates that R_a increased after crosslinking with XDC and quaternization by MI.

Effects of the PEI Concentration and Coating Time on the Filtration Performance

To optimize the PEI concentration, membranes were modified by the polymer in the range $5\text{--}30\ \text{g/L}$, and PEI deposition was physically applied to the PSf UF membrane. As a result, when the PEI concentration was increased, the permeability coefficient

and CaCl_2 rejection were increased (Figure 7). At low concentrations of PEI solution in water, the active layer formation was not good, and just sublayer pores were involved, so this did not have an effect on the rejection, and the permeability coefficient of the membrane decreased dramatically. When the PEI concentration was increased up to $25\ \text{g/L}$, the top layer was formed on a higher level; this was the best active layer with the best permeability coefficient. Moreover, CaCl_2 rejection was $4.6\ \text{L m}^{-2}\ \text{h}^{-1}\ \text{bar}^{-1}$ and 87%, respectively. With a further increase in the PEI concentration, the thickness of top layer was enhanced, and this led to a decrease in the permeability coefficient. Finally, the best concentration was obtained at $25\ \text{g/L}$.

In the next step, the best remaining time of the PSf membrane in PEI aqueous solution was measured with the best concentration. As expected, with the passage of time, PEI was better mixed with the PSf UF membrane. For the first time ($0.0005\ \text{h} < 2\ \text{s}$), the PSf membrane was immersed in PEI solution for a moment. Figure 8 shows that with increasing coating time, the permeability coefficient was decreased, and the rejection was increased. For example, at $0.5\ \text{h}$, the permeability coefficient and rejection were $9.61\ \text{L m}^{-2}\ \text{h}^{-1}\ \text{bar}^{-1}$ and 61%, respectively, and at $1\ \text{h}$, they were $5.1\ \text{L m}^{-2}\ \text{h}^{-1}\ \text{bar}^{-1}$ and 87.8%, respectively. As shown in Figure 8, after $1\ \text{h}$, the conditions remained almost constant. So, the best time for coating PEI on the PSf UF membrane was $1\ \text{h}$.

Effects of the XDC Concentration on the Filtration Performance

Figure 9 shows the effect of the XDC crosslinker concentration on the membrane filtration performance. The results show that

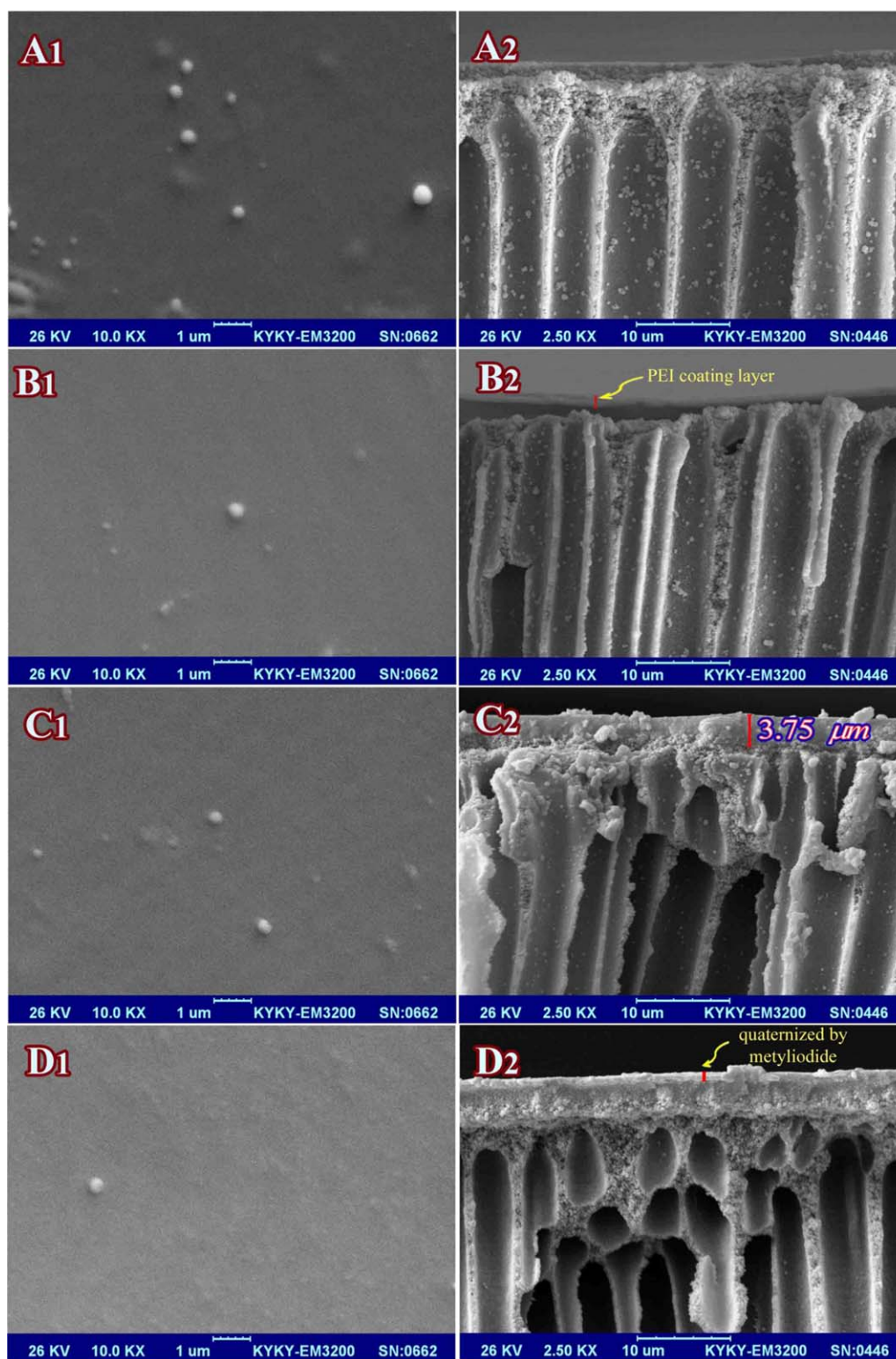


Figure 5. SEM images of the surfaces (set 1) and cross sections (set 2) of the membranes: (A) PSf UF support, (B) membrane coated with PEI, (C) membrane with crosslinked XDC, and (D) NF membrane quaternized with MI. [Color figure can be viewed in the online issue, which is available at wileyonlinelibrary.com.]

with an increase in XDC concentration from 1 to 5 g/L, the CaCl_2 rejection and permeability coefficient of the coated membrane increased. After that, with further increasing concentration, the rejections and permeability decreased. These results

might be due to the fact that when the XDC concentration exceeded the crosslinking reaction stoichiometry of 1:2 between the XDC molecules and amino groups of PEI, the more XDC did not play the role of crosslinking.^{12,20} This could have been

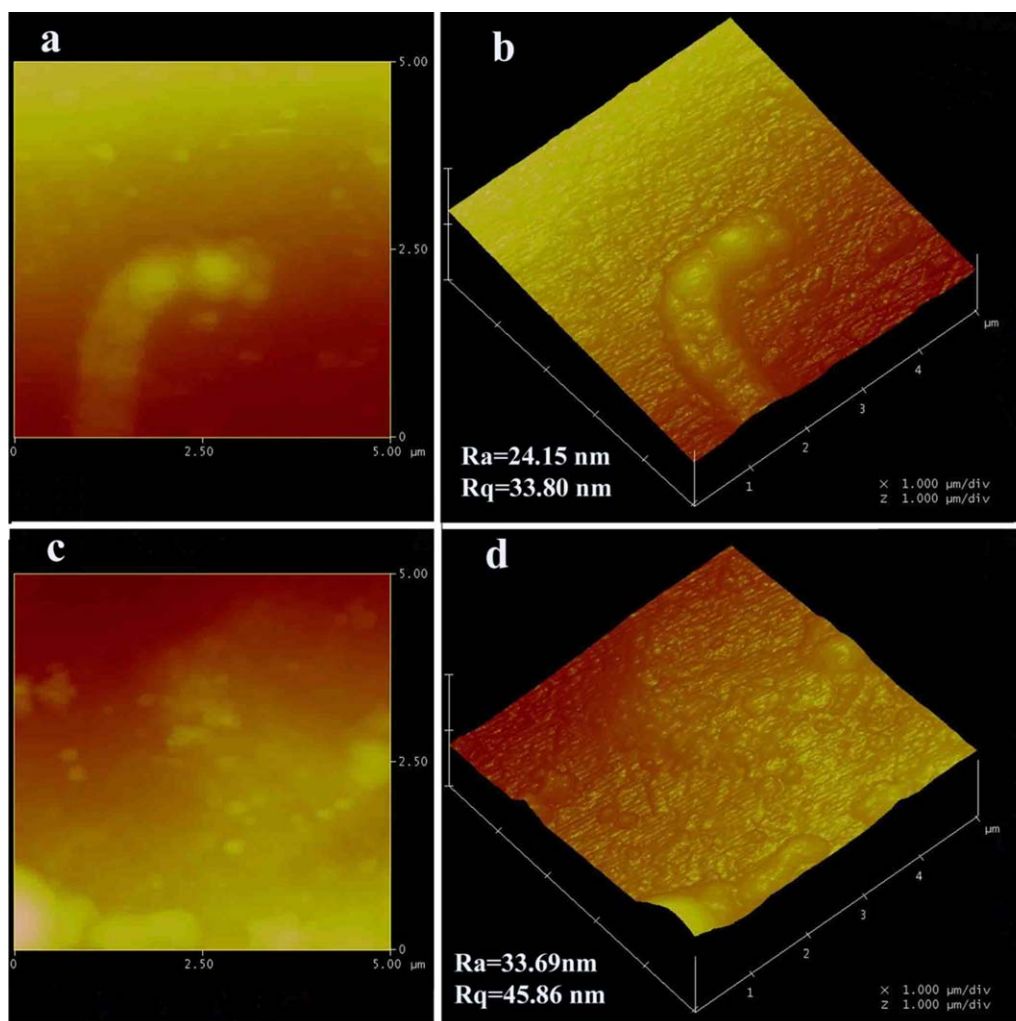


Figure 6. Two- and three-dimensional AFM images of the (a,b) support membrane and (c,d) quaternization membrane by CH_3I . R_q = root mean square roughness. [Color figure can be viewed in the online issue, which is available at wileyonlinelibrary.com.]

due to the improvement in the degree of chemical quaternization crosslinking reaction between PEI and XDC; this happened as a result of the increasing XDC concentration.

Quaternization of PEI on the Top Layer and the Effect of the MI Concentration on the Filtration Performance

As shown in Figure 1,²⁰ amines on the PEI can receive an R^+ covalent bond, and this leads to PEI quaternization. In this

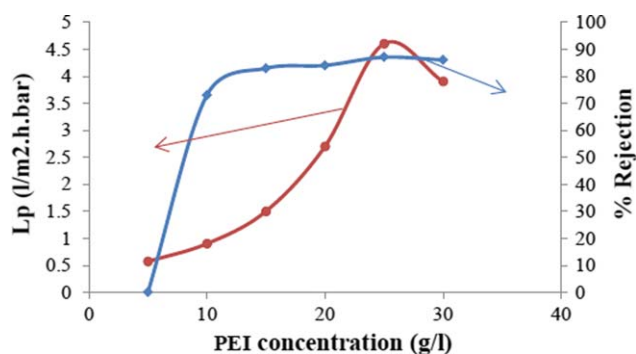


Figure 7. Effect of the PEI concentration on the rejection and permeability coefficient (coating time = 120 min, [XDC] = 5 g/L, crosslinking time = 300 min, pressure = 4 bars, temperature = $25 \pm 2^\circ\text{C}$). [Color figure can be viewed in the online issue, which is available at wileyonlinelibrary.com.]

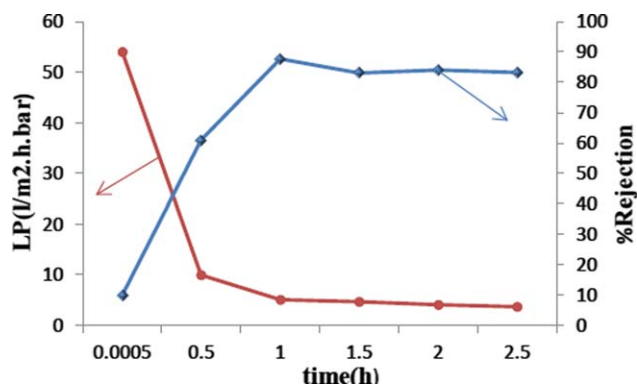


Figure 8. Effect of the coating time on the rejection and permeability coefficient ([PEI] = 25 g/L, [XDC] = 5 g/L, crosslinking time = 300 min, pressure = 4 bars, temperature = $25 \pm 2^\circ\text{C}$). [Color figure can be viewed in the online issue, which is available at wileyonlinelibrary.com.]

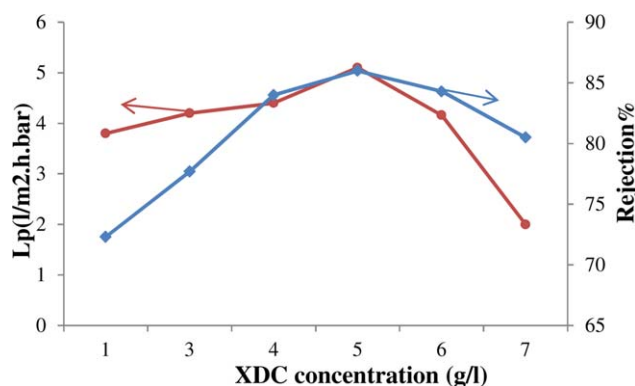


Figure 9. Effect of the XDC concentration on the rejection and permeability coefficient ([PEI] = 25 g/L, coating time = 60 min, crosslinking time = 300 min, pressure = 4 bars, temperature = $25 \pm 2^\circ\text{C}$). [Color figure can be viewed in the online issue, which is available at wileyonlinelibrary.com.]

study, MI was applied to form quaternary ammonium groups because of the short substituent combination and good reactivity. In this reaction, CH_3^+ groups were in competition with protons (H^+); therefore, the membrane stayed in an NaOH aqueous solution (0.25M) for a few minutes after the crosslinking reaction. To obtain the best concentration of MI solution in ethanol, first the membranes were modified, coated with 25 g/L PEI for 1 h and with 5 g/L XDC for crosslinking for 5 h. The second stage of modification and quaternization was carried out with four concentrations (2, 4, 8, and 16% v/v). Figure 10 shows the effect of the MI concentration on the membrane filtration performance. When the MI concentration was enhanced from 2 to 16% v/v, the CaCl_2 rejection of the membrane increased, but there was a slight decline in the permeability coefficient. According to the results, the best concentration of MI for cauterization was 4% v/v because, at this concentration, the salt rejection increased up to 93%, but there was significant decrease in the permeability.

MWCO Calculation

Figure 11 illustrates the rejection curves of the PEI/PSf membranes for PEG solutions with different molecular weights. The

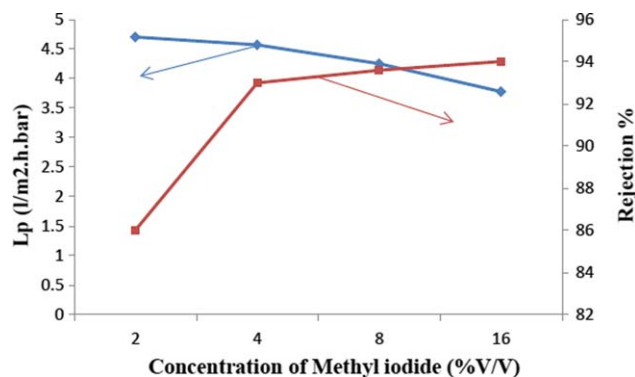


Figure 10. Effect of the MI concentration on the rejection and permeability coefficient ([PEI] = 25 g/L, coating time = 60 min, [XDC] = 5 g/L, crosslinking time = 300 min, pressure = 4 bars, temperature = $25 \pm 2^\circ\text{C}$). [Color figure can be viewed in the online issue, which is available at wileyonlinelibrary.com.]

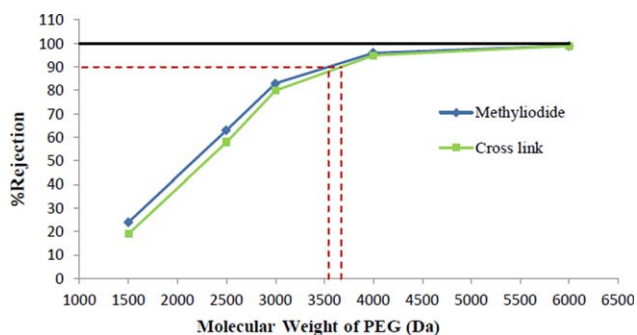


Figure 11. Rejection of the PEG solutions with different molecular weights by the crosslinked and quaternized membranes ([PEI] = 25 g/L, coating time = 60 min, [XDC] = 5 g/L, crosslinking time = 300 min, [MI] = 4% V/V, quaternization time = 120 min, pressure = 4 bars, temperature = $25 \pm 2^\circ\text{C}$). [Color figure can be viewed in the online issue, which is available at wileyonlinelibrary.com.]

MWCO value refers to the molecular weight of PEG that was rejected by the membrane by 90%. The membrane pore size was estimated with the relationship between the MWCO obtained by the PEG solutions and the corresponding radius of the pores calculated by eq. (4).²⁶ The MWCO of the PSf NF membranes was evaluated with five different feed aqueous solutions of PEG (500 ppm) with molecular weights of 1500, 2000, 3000, 4000, and 6000 Da.

According to the results, for the final two membranes, one was just crosslinked PEI by p-xylene dichloride (XDC), and the other one was quaternized by a 4% v/v solution of MI, and the MWCOs were estimated to be 3670 and 3540, which corresponded to 1.49- and 1.47-nm pore radii, respectively.

Rejection of Different Inorganic Salts by the PEI/PSf NF Membrane

The salt rejection of membranes was examined for different inorganic salt solutions (Na_2SO_4 , MgSO_4 , NaCl, and CaCl_2) with a concentration of 1000 ppm at 25°C and 4 bars. The results are shown in Figure 12. The order of rejection for different salt solutions was as follows: $\text{Na}_2\text{SO}_4 < \text{MgSO}_4 < \text{NaCl} < \text{CaCl}_2$. This

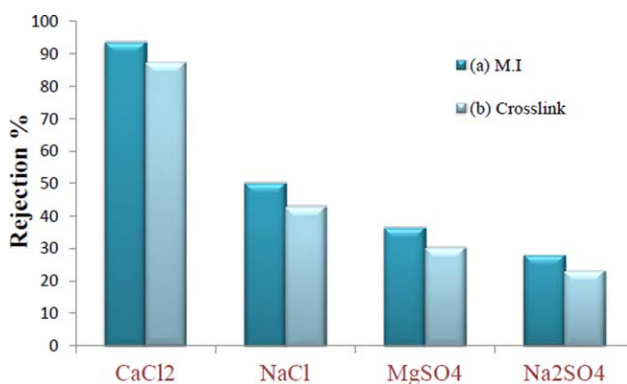


Figure 12. Salt rejection of the PSf NF membranes with different salt solutions: (a) quaternized with MI after crosslinking and (b) crosslinked with XDC. [Color figure can be viewed in the online issue, which is available at wileyonlinelibrary.com.]

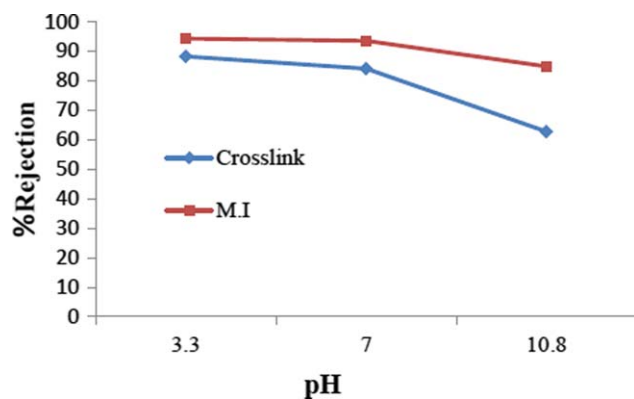


Figure 13. Effect of the feed solution pH on the membrane rejection of CaCl_2 . [Color figure can be viewed in the online issue, which is available at wileyonlinelibrary.com.]

order was justified by the positively charged NF membranes.²⁵ Generally, the PEI-coated PSf NF membranes had a higher rejection for high-valence cations (Ca^{2+}) and low-valence anions (Cl^-) than for low-valence cations (Na^+) and high-valence anions (SO_4^{2-}). According to the Donnan exclusion theory,⁸ this was due to the stronger electrostatic repulsive interaction between high-valence cations and the quaternary ammonium N^+ of the PEI coating of the PSf NF membrane surface. Cations or anions did not exist alone in the aqueous solution; this means that any cations were covered with anions and vice versa. However, according to the Donnan exclusion theory, there was some anionic attraction, and these ions passed through the membrane.

These results indicate that quaternization by MI after the cross-linking process improved the rejection for every inorganic salt solution; this proved that the salt rejection of the charged NF membrane not only was related to the membrane pore size but also mostly depended on the electrostatic repellent interaction between the membrane and cations in the solution.

Effect of the Feed Solution pH on Membrane Rejection

The solution pH appeared to be a major parameter governing the rejection of boron by the two NF membranes selected in this study (Figure 13). Figure 13 shows the changes in the salt rejection of membranes for different pHs (3.3, 7, and 10.8) of the feed solution. The pH was adjusted by the addition of NaOH and HCl to the feed solution. In this case, the membranes were assessed by different pH solutions of CaCl_2 . The results reported in Figure 13 systematically demonstrate the significance of electrostatic interaction and CaCl_2 rejection by the NF membranes. Also, variations in the salt rejection were apparently due to Donnan exclusion change rather than structural changes in the surface layer. Salt rejection decreased at pH 10.8 from 88 to 62.7%, but for the quaternization membrane by MI, the rejection loss was less than that of the crosslinked membrane, from 94.1 to 84.4%, respectively. This finding shows that the quaternized membrane had a more stable surface charge.

Finally, in comparing this study with earlier work, the flux in this experiment occurred at a lower operating pressure than in another's work; also, the PEI used in this study had the clip

to create a more positive charge and was more easily accessible.¹⁹ The structure, surface morphology, and cross section of the membrane were more uniform compared to those in other laboratory work done.¹²

CONCLUSIONS

A novel, positively charged NF membrane was successfully prepared by the coating of PEI on the PSf UF membrane, cross-linking by XDC, and quaternization by MI. The rejection of bivalence inorganic ions was greater than that of monovalent ions. The membrane had a good selective separation properties. The order of salt rejection for inorganic salts was as follows: $\text{CaCl}_2 > \text{NaCl} > \text{MgSO}_4 > \text{Na}_2\text{SO}_4$. With a neutral acidity solution, the membrane exhibited a fairly stable water flux and rejection, but in an acidic or basic environment, the salt rejections changed. In the acidity solution, the charge of membrane was more positive and the rejection increased, and in the basic solution, the surface lost some positive charges, so the rejection decreased. The cross-sectional SEM image confirmed the formation of a thin layer with a thickness of around 3.75 μm . The MWCO determination revealed that the prepared membrane was an NF membrane because the calculated stoke radii was equal to 1.47 nm. Finally, according to the pH tests, the prepared NF membrane surface charge remained constant because the salt rejection at different pH solutions was fixed. The advantages of this technique were the ease of the preparation methods, surface smoothness, good water flux, and high salt retention.

REFERENCES

- Bowen, W. R.; Mohammad, A. W.; Hilal, N. *J. Membr. Sci.* **1997**, *126*, 91.
- Rahimpour, A.; Jahanshahi, M.; Mortazavian, N.; Madaeni, S. S.; Mansourpanah, Y. *Appl. Surf. Sci.* **2010**, *256*, 1657.
- Van der Bruggen, B.; Manttari, M.; Nystrom, M. *Sep. Purif. Technol.* **2008**, *63*, 251.
- Wang, X. L.; Tsuru, T.; Nakao, S.; Kimura, S. *J. Membr. Sci.* **1995**, *103*, 117.
- Schaep, J.; Vandecasteele, C. *J. Membr. Sci.* **2001**, *188*, 129.
- Raman, L. P.; Cheryan, M.; Rajagopalan, N. *Chem. Eng. Prog.* **1994**, *3*, 68.
- Qifeng, Z.; Haifeng, W.; Suobo, Z.; Lei, D. *J. Membr. Sci.* **2011**, *375*, 191.
- Petersen, R. J. *J. Membr. Sci.* **1993**, *83*, 81.
- Zhang, L. L.; Zhang, X. S. *J. Membr. Sci.* **2009**, *33*, 133.
- Akbari, A.; Desclaux, S.; Rouch, J. C.; Aptel, P.; Remigy, J. C. *J. Membr. Sci.* **2006**, *286*, 342.
- Akbari, A.; Desclaux, S.; Rouch, J. C.; Remigy, J. C. *J. Membr. Sci.* **2007**, *297*, 243.
- Lin, L. X.; Li, P. Z.; You, Y. X.; Zhuan, Y.; Bao, K. Z. *J. Membr. Sci.* **2011**, *374*, 33.
- Zhao, Z. P.; Li, J.; Zhang, D. X.; Chen, C. X. *J. Membr. Sci.* **2004**, *232*, 1.

14. Kravets, L.; Dmitriev, S.; Lizunov, N.; Satulu, V.; Mitu, B.; Dinescu, G. *J. Nucl. Instrum. Methods Phys. Res. Sect. B* **2010**, 485.
15. Huang, R. H.; Chen, G. H.; Sun, M. K.; Hu, Y. M.; Gao, C. *J. Membr. Sci.* **2006**, 286, 237.
16. Huang, R. H.; Chen, G. H.; Sun, M. K.; Gao, C. *J. Desalination* **2009**, 239, 38.
17. Wei, X. Z.; Zhu, L. P.; Deng, H. Y.; Xu, Y. Y.; Zhu, B. K.; Huang, Z. *J. Membr. Sci.* **2008**, 323, 278.
18. Yen, C. C.; Yi, Z. H.; Ruoh, C. R.; Ching, J. C.; Kuo, L. T. *J. Membr. Sci.* **2009**, 326, 19.
19. Du, R.; Zhao, J. *J. Membr. Sci.* **2004**, 239, 183.
20. Yun, F. Y.; Ling, S. W.; Zhi, K. X. *J. Membr. Sci.* **2009**, 337, 70.
21. Tian, X.; Kovoichich, M.; Liong, M.; Meng, H.; Kabehie, S.; Zink, J. I.; Andre, E. N. *J. Mater. Chem.* **2007**, 17, 2561.
22. Xiaoliang, W.; Linzhu, Z.; Yongjie, M.; Xu, L.; Hongchen, G. *Nano Res.* **2009**, 2, 365.
23. Tripathy, T.; Ranjan De, B. *J. Phys. Sci.* **2006**, 10, 87.
24. Gao, C.; Yan, D. *Prog. Polym. Sci.* **2004**, 29, 183.
25. Afonso, M. D.; Hagemeyer, G.; Gimbel, R. *Sep. Purif. Technol.* **2001**, 22, 529.
26. Pei, S. Z.; Widjojo, N.; Tai, S. C.; Weber, M.; Maletzko, C. *J. Membr. Sci.* **2012**, 417, 52.